UC Irvine
UC Irvine Previously Published Works

Title
Influence of laser wavelength and pulse duration on gas bubble formation in blood filled glass capillaries

Permalink
https://escholarship.org/uc/item/75t4q6c6

Journal
Laser. Surg. Med., 36(4)

Authors
Choi, B
Kimel, S
Svaasand, LO
et al.

Publication Date
2005-04-01

Copyright Information
This work is made available under the terms of a Creative Commons Attribution License, availalbe at https://creativecommons.org/licenses/by/4.0/

Peer reviewed

eScholarship.org Powered by the California Digital Library
University of California

Lasers in Surgery and Medicine 36:281–288 (2005)

Influence of Laser Wavelength and Pulse Duration on Gas Bubble Formation in Blood Filled Glass Capillaries

Sol Kimel, PhD,[1,2] Bernard Choi, PhD,[1] Lars O. Svaasand, PhD,[1,3] Justin Lotfi,[4] John A. Viator, PhD,[1,5] and J. Stuart Nelson, MD, PhD[1]*

[1]*Beckman Laser Institute, University of California, Irvine, California 92612*
[2]*Department of Chemistry, Technion–Israel Institute of Technology, Haifa 32000, Israel*
[3]*Norwegian University of Science and Technology, Trondheim N-7491, Norway*
[4]*School of Biological Sciences, University of California, Irvine, California 92697*
[5]*Department of Dermatology, Oregon Health Sciences University, Portland, Oregon 97201*

Background and Objectives: Hypervascular skin lesions (HVSL) are treated with medical lasers characterized by a variety of parameters such as wavelength λ, pulse duration t_p, and radiant exposure E that can be adjusted for different pathology and blood vessel size. Treatment parameters have been optimized assuming constant optical properties of blood during laser photocoagulation. However, recent studies suggest that this assumption may not always be true. Our objective was to quantify thermally induced changes in blood that occur during irradiation using standard laser parameters.

Study Design/Materials and Methods: Glass capillary tubes (diameter D = 100, 200, and 337 μm) filled with fresh or hemolyzed rabbit blood were irradiated once at $\lambda = 585$, 595, or 600 nm, $t_p = 1.5$ milliseconds; and also at $\lambda = 585$ nm, $t_p = 0.45$ milliseconds. E was increased until blood ablation caused formation of permanent gas bubbles. In a corroborative study, human blood was heated at 50°C and absorbance spectra were measured as a function of time.

Results: Threshold radiant exposure, E_{thresh}, for gas bubble formation was found not to depend on λ, which might be surprising in view of the 10-fold lower absorption coefficient at 600 nm as compared to 585 nm. The spectroscopic study revealed heat-induced changes in blood constituent composition of hemoglobins (Hb) from initially 100% oxyhemoglobin (HbO_2) to deoxyhemoglobin (HHb) and, ultimately, methemoglobin (metHb) as the major constituent. Model calculations of $E_{thresh}(\lambda,D)$ based on changing constituent blood composition during heating with milliseconds lasers were found to correlate with experimental results.

Conclusions: For laser treatment of HVSL it appears that λ is of secondary importance and that the choice of t_p is a more important factor. Lasers Surg. Med. 36:281–288, 2005. © 2005 Wiley-Liss, Inc.

Key words: blood spectroscopy; bubble formation; laser heated blood; methemoglobin production; port wine stains; selective photothermolysis

INTRODUCTION

Pulsed dye lasers (PDLs) are currently used extensively to treat hypervascular skin lesions (HVSL) such as port wine stain (PWS) birthmarks [1–3], telangiectasias [4], and hemangiomas [5]. PDL parameters are selected to induce permanent photocoagulation of blood and vessel wall damage through conversion of selectively absorbed radiant energy into thermal energy [6].

Laser wavelength, λ is chosen to achieve optimal absorption in blood [7,8]. When optical scattering can be neglected, λ determines the optical penetration depth, $\delta(\lambda) = 1/\mu_a(\lambda)$, where $\mu_a(\lambda)$ is the wavelength-dependent absorption coefficient. Pulse duration, t_p, is selected to allow sufficient heat diffusion into the vessel wall, but not into the adjacent perivascular tissues [9–14]. Most PDLs used in the clinic emit at 585 or 595 nm and have pulse durations of 0.45 or 1.5 milliseconds. Vessels are destroyed by blood coagulation and thermal denaturation of the wall as a result of heating to ~70°C (for t_p in the milliseconds domain) while leaving perivascular tissues below this "threshold" damage temperature [11–15]. With increasing radiant exposure E, photothermal effects progress in the following order: coagulation, aggregated coagulum formation, and bubble formation (i.e., ablation) [16].

Several photothermal in vitro [16–19] and in vivo [8,9,11,20–26] studies have observed that during heating, blood undergoes transient or irreversible biophysical events that may have a significant impact on treatment outcome [16–26]. During slow heating, red blood cells (RBCs) change shape from discs to spheres, followed by membrane denaturation, formation of holes, and egress of hemoglobins (Hb), all of which change the scattering properties of blood [27]. During fast (miliseconds time domain) heating, formation of stationary gas bubbles (in blood) [27] to be distinguished from collapsing vapor bubbles in water [28,29] has been observed, in addition to changes in optical properties of blood [16–24].

Contract grant sponsor: NIH; Contract grant numbers: AR47551, AR48458.
*Correspondence to: J.S. Nelson, MD, PhD, Beckman Laser Institute, University of California, Irvine, 1002 Health Sciences Rd East, Irvine CA 92612. E-mail: snelson@laser.bli.uci.edu
Accepted 14 January 2005
Published online 24 March 2005 in Wiley InterScience (www.interscience.wiley.com).
DOI 10.1002/lsm.20154

© 2005 Wiley-Liss, Inc.

The purpose of this study is to investigate the effects of PDL parameters on gas bubble formation in an in vitro blood vessel phantom. Glass capillaries were used to simulate microvessels. We acknowledge that a salient difference between static blood in glass capillaries and that flowing in vessels in vivo is that coagula, attached to the superficial inner vessel wall, contribute to blood flow obstruction. Also, blood vessels in vivo exposed to PDL have been observed to undergo fast dilatation, leakage, as well as gas bubble formation [17,18,20,25]. The present study presents a quantitative analysis of blood ablation and gas bubble formation in glass capillaries as a function of λ, t_p, E, and lumen diameter D. It is less relevant for understanding heat-triggered denaturation of vessel walls.

MATERIALS AND METHODS

Blood

Blood was drawn from the ear vein of male New Zealand white rabbits, in compliance with Animal Care Regulations at University of California, Irvine, and collected in glass vials coated with ethylenediamine tetraacetic acid (EDTA) anticoagulant. Blood was used either immediately, or after one freeze/thaw cycle that induced RBC hemolysis, as confirmed by microscopic analysis. Hemolyzed blood lacks local inhomogeneities in light absorption, as found in whole blood due to encapsulation of Hb in RBC, while preserving the spectroscopic characteristics of Hb molecules.

Glass Capillary Tubes

We used the smallest commercially available machine-made capillaries to obtain reproducible values for D. Capillaries more comparable to PWS lumen diameters ($D = 20–60$ μm) were not commercially available. Measured D and wall thickness ΔD were:

$D = 100$ μm, $\Delta D = 240$ μm (Drummond Scientific Company, Broomall, PA, N-51-A, borosilicate glass).
$D = 200$ μm, $\Delta D = 230$ μm (Drummond Scientific Company, N-51-A, borosilicate glass).
$D = 337$ μm, $\Delta D = 590$ μm (Kimble #71940 Kontes, Vineland, NJ, soda-lime glass).

Note that for the glass capillaries used, $\Delta D/D$ values ranged from 1.1 to 2.4, whereas for blood vessels $\Delta D/D \sim 0.1$.

Lasers

We employed two flashlamp pumped PDLs used by clinicians to treat HVSL.

1. ScleroPlus™ (Candela Corp., Wayland, MA) with user-specified wavelengths ($\lambda = 585$, 590, 595, or 600 nm), fixed pulse duration, $t_p = 1.5$ milliseconds, and adjustable E.
2. CBeam™ (Candela) with $\lambda = 585$ nm, $t_p = 0.45$ milliseconds, and adjustable E.

Both lasers were used without cryogen spray cooling, with a handpiece producing a 7 mm diameter flat-top beam profile [11].

Experimental Protocol

Capillary tubes were dipped into a vial containing fresh blood, which allowed blood to rise through capillary action to a height of 15–20 mm. Before dipping, the vial was shaken gently to ascertain sample homogeneity. Individual capillaries were then fixed on a glass plate and covered with glycerol (for refractive index matching to the capillary wall, to reduce refraction of incident laser radiation). The laser handpiece was positioned so that the central part of the blood column in each capillary was irradiated in the exact same geometry.

To estimate the threshold radiant exposure (E_{thresh}) required for a 50% probability of bubble formation, probit analysis was used [30]. For each E, the presence or absence of bubble formation was documented photographically. The percent occurrence of bubble formation was plotted versus log(E) and a sigmoidal curve fitted to the data, using Prism 4 software (GraphPad Software, Inc., San Diego, CA). E_{thresh} and 95% confidence intervals were determined from the curve fit.

All experiments were repeated with hemolyzed blood, in which Hb are homogeneously distributed rather than concentrated in RBCs.

Documentation

Photographic documentation allowed determination of the number and position of gas bubbles formed at both ends of the capillary, placed alongside a ruler (Fig. 1). The set-up consisted of a still camera (Olympus, model C-35AD) mounted on a stereomicroscope (model M5A, Wild, Switzerland), operated with an exposure control unit (Olympus). The microscope was equipped with an extra lens ($0.75\times$) that enlarged the field of view to a diameter of 4 cm, to allow observation of gas bubbles formed on both sides of the blood

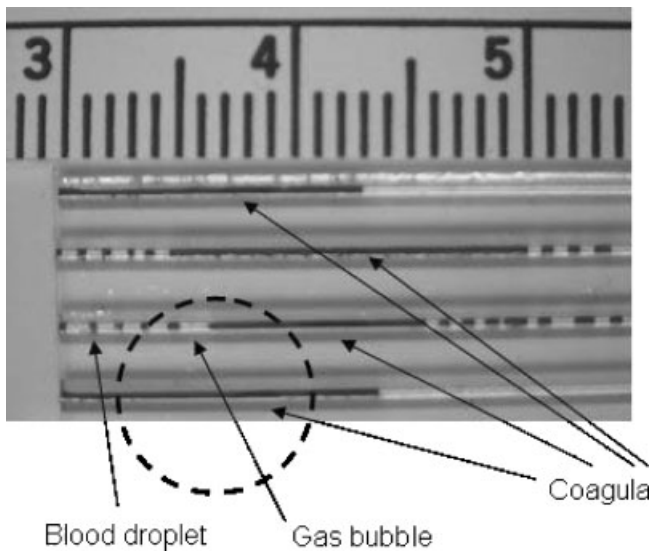


Fig. 1. Capillaries ($D = 337$ μm) filled with hemolyzed blood after irradiation at E_{thresh} with the ScleroPlus laser ($\lambda = 585$ nm, $t_p = 1.5$ milliseconds, $E = 6$ J/cm^2). Gas bubble formation is evident in the middle two capillaries.

column in the capillary. Care was taken to maintain constant lighting and exposure conditions.

Increasing Methemoglobin (metHb) Content

The metHb concentration in blood was increased by preheating sealed vials, containing human blood from a healthy donor, to 50°C with a water bath. After selected time intervals (up to 4.5 hours), samples were withdrawn from the vials, hemolyzed with ammonium chloride, 8.3 g/L (Sigma Chemical Co., St. Louis, MO) and diluted 200-fold with distilled water. Shortly thereafter, the absorption spectrum was measured between 550 and 700 nm with a Beckman DU600 spectrophotometer, and again 12 hours later to ascertain the stability of the metHb formed.

To estimate E_{thresh} of metHb containing blood, we preheated blood for 150 minutes at 50°C to generate metHb and subsequently allowed it to cool to 25°C. We repeated the experimental protocol described above using the ScleroPlus laser and irradiating simultaneously pairs of 200 μm diameter capillaries, one filled with preheated blood (i.e., containing mostly metHb), and the other with fresh blood (i.e., containing predominantly oxyhemoglobin (HbO_2)). Wavelengths of 585 and 600 nm were used in this set of experiments.

RESULTS

Microscopic video recording immediately after PDL exposures at $E = E_{thresh}$ revealed gas microbubbles, which coalesced into macrobubbles after about 500 milliseconds, yielding at both ends of the capillary tube a periodic pattern of 3–10 macrobubbles, each separated by approximately 1–2 mm of blood. The gas bubbles did not collapse after the blood cooled, as would be expected if water vapor had been the main constituent [28,29]. The ratio of gas bubbles volume to blood volume was about 20%, as is expected if most of the Hb-bound oxygen was released as gas during the laser pulse.

Figure 1 is a color photograph showing four representative 337 μm diameter capillaries, each (individually) irradiated at E_{thresh}.

Figure 2 presents a graph of $E_{thresh}(\lambda,D)$ determined through probit analysis [30], using the ScleroPlus laser, with $\lambda = 585$, 595, and 600 nm, and $t_p = 1.5$ milliseconds. Error bars represent the 95% confidence intervals of $\log(E_{thresh})$. It should be noted that the spread in the probabilities of the mean values may be quite large.

Figure 3 shows results for $E_{thresh}(D)$ for hemolyzed blood irradiated with the CBeam laser at $\lambda = 585$ nm and $t_p = 0.45$ milliseconds, for different values of D.

Spectra of hemolyzed human blood were measured after heating for up to 270 minutes at 50°C, a temperature chosen since ultrastructural changes of RBCs are known to occur [17]. The metHb fraction at selected times was determined from the corresponding ratio of absorbances at 585 and 600 nm. A typical absorbance spectrum obtained after preheating whole venous blood for 270 minutes is shown in Figure 4; the metHb band around 630 nm is clearly discernible. Relative absorbances for shorter heating times are given in Table 2, rows 1 and 2.

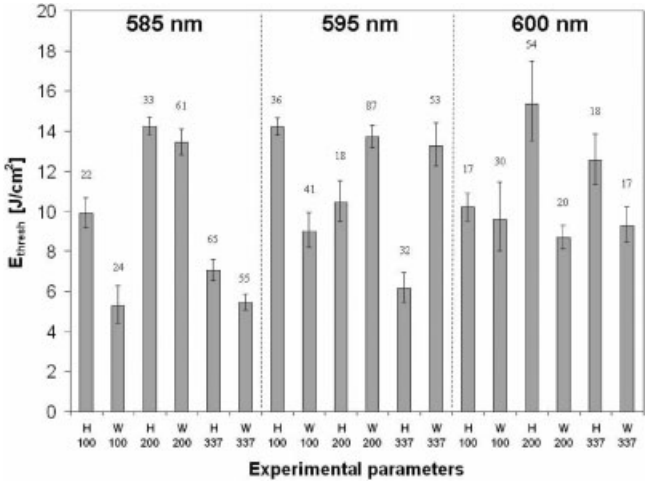


Fig. 2. Measurements of E_{thresh} for the ScleroPlus laser at $t_p = 1.5$ milliseconds for different values of λ and D. H, hemolyzed blood; W, whole blood; n, number of experiments. Error bars represent the 95% confidence intervals of $\log(E_{thresh})$.

Pairs of capillaries ($D = 200$ μm), one filled with preheated blood (150 minutes at 50°C) and another containing fresh blood (both at room temperature) were irradiated with the ScleroPlus laser ($t_p = 1.5$ milliseconds) and compared. With 585 nm irradiation, gas bubble formation was consistently more pronounced for fresh blood than for preheated blood. A contributing factor may be the increased viscosity observed in blood following prolonged preheating at 50°C. Values of E_{thresh} were 9 and 10.5 J/cm^2 for fresh and preheated blood, respectively, whereas at 600 nm, corresponding E_{thresh} values were 12.5 and 13.5 J/cm^2. At 600 nm, the extent of gas bubble formation was fairly similar for both experimental conditions, presumably due to the initial more uniform heating (and thus more uniform

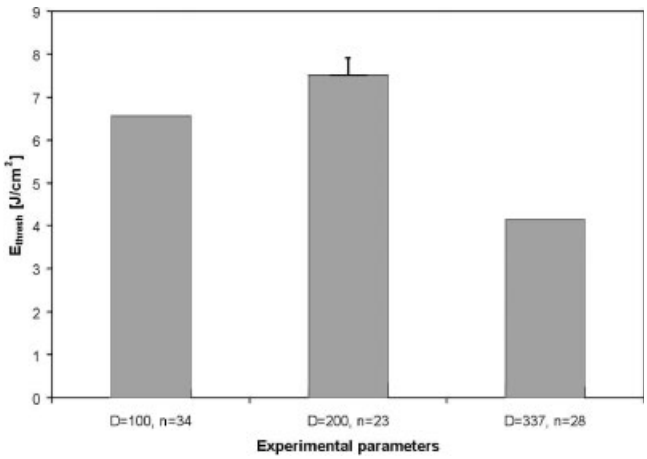


Fig. 3. E_{thresh} measurements on hemolyzed blood with the CBeam laser at $\lambda = 585$ nm and $t_p = 0.45$ milliseconds.

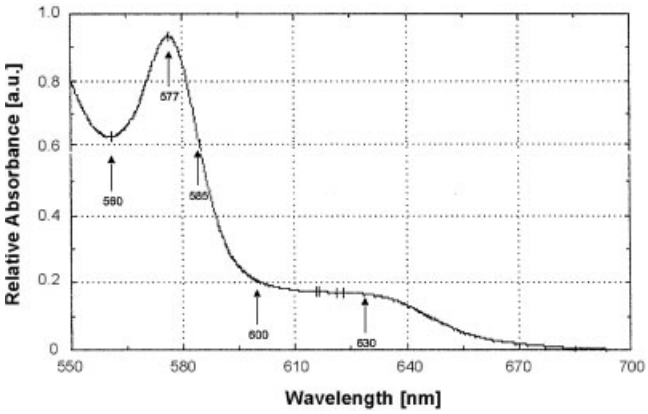


Fig. 4. Absorbance spectrum of hemolyzed human blood at room temperature (preheated for 270 minutes at 50°C). Arrows specify relevant wavelengths.

TABLE 1. *P*-Values for E_{thresh} of Hemolyzed Versus Whole Blood for Different Values of Wavelength and Capillary Diameter

λ (nm)	D (μm)	*P*-value
585	100	<0.0001
585	200	0.0674
585	337	<0.0001
595	100	<0.0001
595	200	<0.0001
595	337	<0.0001
600	100	0.5835
600	200	<0.0001
600	337	0.0001

oxygen release) across the capillary lumen compared to that at 585 nm.

DISCUSSION

In whole blood, Hb are concentrated in RBCs, whereas in hemolyzed blood, Hb are homogeneously distributed. During irradiation, encapsulated Hb may act as local nucleation sites for gas bubble formation, allowing for more efficient conversion of incident laser energy to kinetic energy necessary for macrobubble generation. Thus, one might expect a lower E_{thresh} for whole blood. However, the difference will not be large as the diffusion length for a 1.5 milliseconds laser pulse is about 13 μm, so that most of the absorbed energy will diffuse out of the erythrocyte during a pulse. Indeed, statistical analysis of the nine experimental conditions in Figure 2 shows that in seven out of nine cases $E_{thresh}(\lambda D)$ was lower for whole than for hemolyzed blood. *P*-values are given in Table 1.

Modeling

The substantial difference in $E_{thresh}(\lambda)$ that would have been expected if the temperature rise had been determined exclusively by $\mu_a(HbO_2)$, is completely absent. The values of $E_{thresh}(\lambda)$, averaged over all values of D, at 585, 595, and 600 nm are, respectively, 8.7, 11.9, and 9.4 J/cm^2. Furthermore, no systematic trend in $E_{thresh}(D)$ at each λ was observed for the three different tube diameters, in spite of the fact that the values of $\delta(\lambda)_{HbO2}$ markedly differ. Even though the results in Figure 2 demonstrate a large statistical variation, it is clear that E_{thresh} is not determined solely by absorption of laser light by HbO_2.

A possible explanation might be that heating and/or photoacoustic stress during the early part of the laser pulse release bound oxygen, resulting in conversion of HbO_2 to deoxyhemoglobin (HHb), which is accompanied by gas bubble formation. Further heating causes oxidation of ferrous Hb (Fe^{2+}) to the ferric state (Fe^{3+}); i.e., to metHb [18], also denoted hemiglobin [31]. If the time dependent absorption is expressed as the sum of absorptions in the three constituents HbO_2, HHb, and metHb, each in its appropriate time domain, the corresponding composite penetration depth δ can be approximated,

$$\delta^{-1} = \int_0^{t_p} \frac{1}{t_p}\left[\left(\frac{\left(1 - aH\left(\frac{t-t_{HHb}}{t_{HHb}}\right) - (1-a)H\left(\frac{t-t_{metHb}}{t_{metHb}}\right)\right)}{\delta_{HbO_2}} + \frac{a\left(H\left(\frac{t-t_{HHb}}{t_{HHb}}\right) - H\left(\frac{t-t_{metHb}}{t_{metHb}}\right)\right)}{\delta_{HHb}} + \frac{bH\left(\frac{t-t_{metHb}}{t_{metHb}}\right)}{\delta_{metHb}}\right)\right] dt$$

where a and b are, respectively, the fractional concentrations of HHb and metHb, while t_{HHb} and t_{metHb} denote times at which these species are formed. Penetration depths for the three constituents are denoted by δ_{HbO2}, δ_{HHb}, and δ_{metHb}. The function H(t) is the Heaviside unit step function defined by $H(t) = 0$ for $t < 0$ and $H(t) = 1$ for $t > 1$.

Note that blood in a glass capillary has an oxygen saturation of approximately 100%. The time points of conversions of HbO_2 to HHb and metHb will depend on λ as well as on irradiance. For simplicity, a is allowed to be unity in the time interval between t_{HHb} and t_{metHb}. At 585 nm and $E \geq E_{thresh}$, conversion to HHb is assumed to occur at time $t_{HHb} = 0.1t_p$, followed by conversion to metHb at time $t_{metHb} = 0.5t_p$. At these times, approximate irradiances for conversion are $0.1E_{thresh} \sim 1$ J/cm^2 and $0.5E_{thresh} \sim 5$ J/cm^2, since to a first approximation, the contour of ScleroPlus laser pulses E(t) is flat [11]. These irradiances can be compared to the threshold values of 4 J/cm^2 (577 nm, 0.36 milliseconds) for morphological changes in RBCs [17] and 2.9 J/cm^2 reported for the temperature-dependent change in effective optical absorption of blood observed during a 585 nm 0.5 milliseconds PDL pulse [18]. A transient 2.5-fold increase

TABLE 2. Relative Absorption of Whole Human Venous Blood Heated to 50°C

Heating time (minutes)	0	45	105	150	210	270
Measured ratio 560/577	0.60 ± 0.01	0.61 ± 0.01	0.65 ± 0.03	0.66	0.72	0.76
Measured ratio 585/600	6.2 ± 0.5	4.2 ± 0.5	2.9 ± 0.5	2.6	2.1	1.7
Calculated metHb fraction (%)	16	34	53	59	70	81
Calculated ratio 560/577	0.60	0.63	0.68	0.70	0.75	0.82

in effective absorption has been detected, in a spatially confined (~20 μm) layer in the cuvette during a short period within the pulse [18]. This may be explained by a variety of effects such as changes in transmittance due to increased scattering because of gas microbubble formation rather than to a phenomenological increase of the absorption coefficient. It is interesting to note that this threshold value was found to be independent of the total E of the pulse as is to be expected when explained in terms of conversion of HbO_2 to HHb and metHb. The second threshold value of 6.3 J/cm^2 reported in that study [18] more closely corresponds to our E_{thresh} values and is caused by rapid expansion of gas macrobubbles due to blood ablation. Based on conversion of the various blood components (see Table 2), the composite penetration depth at $\lambda = 585$ nm accordingly is $\delta \sim 82$ μm.

At 600 nm, the corresponding heating time for conversion to HHb is assumed to be $0.3t_p$, while the time of conversion to metHb remains $0.5t_p$. Thus, at $\lambda = 600$ nm, the composite penetration depth will be $\delta \sim 200$ μm.

In Table 2, the first row gives the ratio between absorbances of preheated human blood at the 560 nm valley and the 577 nm HbO_2 peak (see Fig. 4). This ratio is 0.57 for 100% oxygen saturation [31] and the initial value of the 560/577 ratios indicates that Hb was close to 100% saturated with oxygen. The ratio increased with heating time, indicating a continuous drop in HbO_2 and replacement with HHb and metHb, constituents that absorb in this spectral region without a peak at 577 nm. The second row lists the ratio between the absorbances at 585 and 600 nm. Because of the steep slope around 585 nm, the 585/600 ratios are inherently less accurate than the 560/577 ratios. Based on tabulated values of metHb absorbance (see Table 3), the metHb fraction for all heating exposures could be calculated from the 585/600 ratios, as given in the third row of Table 2. After 105 minutes at 50°C, more than 50% of Hb is converted to metHb. The last row in Table 2 lists calculated values for the ratios 560/577 based on a binary mixture of HbO_2 and metHb.

The satisfying agreement between measured (row 1) and calculated values (row 4) is based on equilibrium values of HbO_2 conversion to metHb, without detection of HHb as an intermediate. This is correct for the experimental protocol used in this study since after heating at 50°C, blood was diluted 200-fold to allow the absorbance to be measured in a standard spectrophotometer, resulting in complete oxygen saturation by oxygen trapped in the solvent.

Table 3 lists the molar extinction coefficient $\varepsilon(\lambda)$ (in units $cm^{-1}M^{-1}$) [31] for the main chromophores in hemolyzed human blood. Data at 577, 585, and 595 nm are found from linear interpolation of tabulated entries at adjacent λ. The isosbestic point is at $\lambda = 586$ nm. The steep slope of $\varepsilon(HbO_2)$ around 585 and 595 nm could substantially influence the amount of absorbed radiant energy and, when λ shifts by as little as ±1 nm, thus in principle also affect the ensuing photophysical events. Table 3 shows that $\varepsilon(HbO_2)$ decreases by one order of magnitude from 585 to 600 nm, whereas ε(HHb) decreases merely by a factor of two over the same wavelength region; in contrast ε(metHb) and thus δ(metHb) are almost the same for 585, 595, and 600 nm.

Similarly, Table 4 lists the optical penetration depth $\delta(\lambda)$ for constituents in hemolyzed blood with a Hb concentration of 150 g/L, equal to that of normal whole blood,

$$\delta(\lambda) = (\mu_a(\lambda))^{-1} = (\varepsilon(\lambda))^{-1}\left(\frac{64{,}500/150}{100(\ln 10)}\right)$$

Based on measured spectra for blood heated to 50°C and the equilibrium metHb fractions determined therein (Table 2, row 3), $\mu_a(\lambda)$ was calculated for different compositions of blood present during heating, as listed in Table 5. As expected, preheating of blood leads to increased E_{thresh} at 585 nm (because of the reduced HbO_2 content) and, in parallel, causes lower E_{thresh} at 600 nm than calculated (see Fig. 5A, upper curve) because of metHb formation. Percent changes of $\mu_a(\lambda)$ listed in Table 5 present trends rather than actual changes since during pulsed laser heating nonlinear effects will occur [17–26].

TABLE 3. Molar Extinction Coefficient ε(λ) ($cm^{-1}M^{-1}$) of Hemolyzed Blood Components According to Zijlstra et al. [31]

λ (nm)	ε(HbO_2)	ε(deoxyhemoglobin (HHb))	ε(methemoglobin (metHb))
560	35,070	52,440	16,700
577	61,240	39,170	16,030
585	36,440	32,480	15,150
595	7,700	21,210	13,410
600	3,840	15,040	12,900

TABLE 4. Optical Penetration Depth δ(λ) (μm) in Hemolyzed Blood Components

λ (nm)	δ(HbO_2)	δ(HHb)	δ(metHb)
585	51	57	123
595	243	88	139
600	486	124	145

Using the Hb conversion dynamics and Equations 1A, 2A (see Appendix), we have calculated radiant exposures E(λ,D) required for heating blood-filled capillaries. The curves in Figure 5 give the required radiant exposure E(λ,D) for heating blood-filled capillary tubes from ambient temperature (25°C) to 100°C.

Experimental results for $E_{thresh}(\lambda,D)$ (Figs. 2 and 5, symbols ●, ■, ◆) indicate that δ in heated blood is about the same for the three wavelengths studied. It is expected that at the beginning of the laser pulse δ is close to the value for HbO_2, but that δ changes as the temperature rise releases bound molecular oxygen thus generating HHb as well as gaseous oxygen. When the temperature approaches 65–75°C, oxidative stresses convert part of Hb to metHb [24–26]. A further rise in temperature will denature the proteins and introduce strongly enhanced scattering. Qualitatively, partial conversion of HbO_2 to HHb and metHb will move the upper and lower curves in Figure 5A toward the middle curve, thus eliminating the discrepancy between measured and calculated $E_{thresh}(\lambda,D)$. Details of the changes in the process are, of course, dependent on the

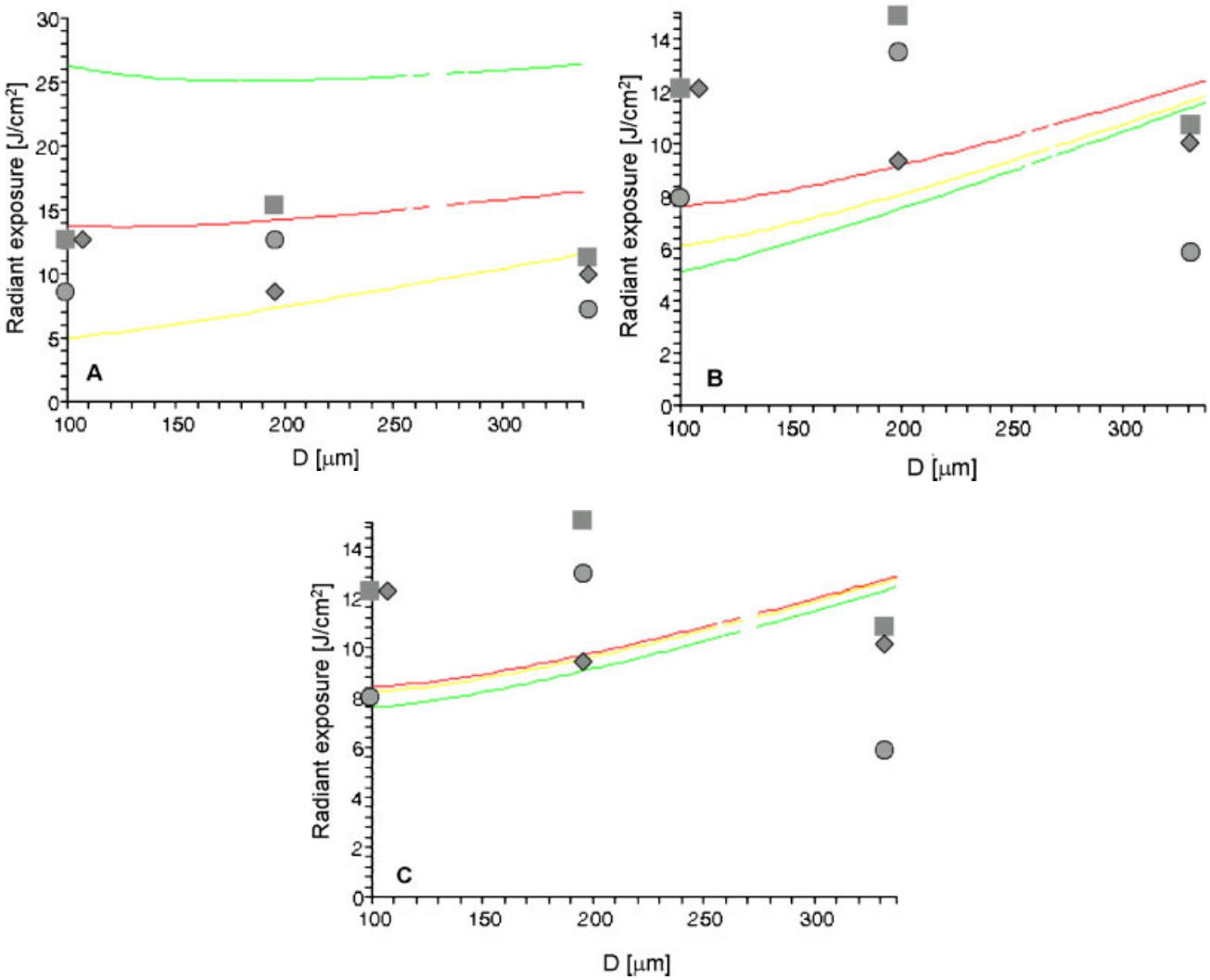


Fig. 5. Calculated radiant exposures E(λ,D) required for heating blood-filled capillary tubes from 25 to 100°C. **Panel A**: Oxyhemoglobin (HbO_2) 100% saturated; **panel B**, deoxyhemoglobin (HHb); **panel C**, methemoglobin (metHb). In all panels, upper curves are for λ = 600 nm, middle curves for 595 nm, and lower curves for 585 nm. Circles, squares, and diamonds represent the average measured E_{thresh} at 585, 595, and 600 nm, respectively. [Figure can be viewed in color online via www.interscience.wiley.com.]

TABLE 5. Change in Absorption Coefficient for Hemolyzed Blood After Different Heating Periods at 50°C

Wavelength (nm)	45 minutes (%)	105 minutes (%)	150 minutes (%)	210 minutes (%)	270 minutes (%)
585	−20	−31	−35	−41	−47
595	+25	+39	+44	+52	+60
600	+80	+125	+139	+165	+191

conversion dynamics. However, based on the conversion dynamics of Hb and on Equations 1A–3A, a best fit to the experimental data presented in Figures 2 and 5 suggests that an effective penetration depth in the range $\delta \approx 100$–200 μm, corresponding to $\mu_a = 5000$–$10{,}000\ m^{-1}$, is valid over the entire wavelength region 585–600 nm.

Values of E_{thresh} observed for $\lambda = 585$ nm and $t_p = 0.45$ milliseconds are shown in Figure 3. For all D values under study, E_{thresh} required to achieve gas bubble formation is higher for 1.5 milliseconds pulses than for 0.45 milliseconds pulses, because more heat is lost to conduction into the glass wall during 1.5 milliseconds than 0.45 milliseconds. The average observed E_{thresh} values for $D = 100$, 200, and 337 μm are, respectively, 6.6, 7.5, and 4.2 J/cm^2, whereas the corresponding calculated values of $E_{thresh}(D)$ are 5.9, 7.9, and 11 J/cm^2.

Calculated E_{thresh} values for $D = 100$ and 200 μm thus correspond well to experimental results, but for $D = 337$ μm, calculated values are significantly higher than measured E_{thresh}. This result might indicate only partial mixing of heated and non-heated blood in the larger capillary tube thus facilitating gas bubble formation, a phenomenon expected to be more pronounced for the shorter 0.45 milliseconds pulses as compared to 1.5 milliseconds pulses.

CONCLUSIONS

The results for $E_{thresh}(\lambda, t_p, D)$ have been interpreted assuming formation of a mixture of HbO_2, HHb, and metHb which changes during fast heating (milliseconds domain) by absorbed optical energy or by slow direct heating. The qualitative agreement of the surprising result obtained for E_{thresh} at 600 nm, i.e., the independence of E_{thresh} on λ, with model calculations is satisfying. However, it should be noted that the agreement between experimental and calculated values of E_{thresh} refers to the glass capillary model. At the same time, the heat-triggered dynamic conversion of HbO_2 to HHb and ultimately to metHb is universal. It represents an important step in HVSL and a better understanding may have clinical relevance. A complete description of HVSL should take into account the cascade of biochemical changes, beyond conversion of blood components, which occur after absorbance of pulsed irradiation.

Also, during pulsed irradiation in the milliseconds domain, non-linear and non-equilibrium processes take place [16–20]. Therefore, more detailed investigations are required.

Among implications for treatment of HVSL, we mention the reduced relevance of choosing the wavelength in medical lasers and the reaffirmed importance of choosing the pulse duration.

ACKNOWLEDGMENTS

BC thanks the Arnold and Mabel Beckman Fellows Program for funding support. Jared Goodman at Brigham Young University assisted in some of the experiments. The authors thank Lise L. Randeberg (Trondheim) and Wim Verkruysse (Irvine) for helpful discussions.

APPENDIX

Numerical Calculation of Laser Heating of Blood

The primary temperature rise occurs at the location of light absorption (essentially within a layer of blood with thickness δ). Convective flow, promoted by microbubble formation, will rapidly equalize the temperature gradient across the vessel lumen [11], though this may not necessarily be true in vessels where $D \gg \delta$. When convective flow conditions are satisfied, the temperature rise is averaged over the entire lumen, and the incremental temperature rise dT at a time t after exposure to irradiance S during the time interval dt can be approximated [3],

$$dT = \frac{\mu_{a,eff}^{dyn} S A dt}{\left(\rho_b C_b A + \rho_g C_g P \sqrt{\chi_g t}\right)} \qquad (1A)$$

Where ρ_b and C_b are, respectively, the density and specific heat per unit mass of blood, whereas ρ_g and C_g are the corresponding values for glass. The cross-sectional area of the capillary lumen $\pi D^2/4$ is denoted A, and $P = \pi D$ is the capillary lumen circumference. The irradiance is given by $S = E/t_p$.

The diffusion distance of heat into the capillary wall during time t is approximately $\sqrt{\chi_g t}$, where χ_g is the thermal diffusivity of glass. The approximation for dT given in Equation 1A is valid provided that this distance is much less than D. The thermal diffusivities for borosilicate glass and blood are 6.6×10^{-7} and 1.2×10^{-7} m^2/second, respectively [32]. Thus, thermal diffusion into the glass wall ($\delta_{thermal} = \sqrt{\chi_g t_p}$) will occur for about 20 and 30 μm for t_p of 0.45 and 1.5 milliseconds, respectively [33]. Incidentally, the fact that $\delta_{thermal} \ll \Delta D$ allows comparison of glass capillaries (wall thickness $\Delta D = 240$–590 μm) with blood vessels with $\Delta D = 20$–30 μm.

The reduced absorption due to optical shielding effects in the deeper regions of the vessel lumen is accounted for by using an effective absorption coefficient $\mu_{a,eff}^{dyn}$ representing the average absorption across the lumen; i.e., the total absorbed power per unit length of the capillary is $\mu_{a,eff}^{dyn}$ SA [8].

The curves in Figure 5 were obtained by integration of Equation 1A over t_p, assuming constant μ_a for each blood

constituent during the entire heating process. The curves might serve as indicative guidelines for the average effective dynamic absorption coefficient $\mu_{a,eff}^{dyn}$ [8,9,11]

$$\mu_{a,eff}^{dyn} = 2\frac{I(1,D/\delta) - L(1,D/\delta)}{D} \quad (2A)$$

where $I(1,D/\delta)$ is the first order modified Bessel-I function and $L(1,D/\delta)$ is the first order Struve function. This expression reduces to $\mu_{a,eff}^{dyn} = \mu_a$ when $\delta \gg D$; i.e., when optical depletion is negligible, and to $\mu_{a,eff}^{dyn} = 4/\pi D$ when $\delta \ll D$; i.e., when all incident light is absorbed. Equation 2A can be approximated by,

$$\mu_{a,eff}^{dyn} \approx 4\frac{1 - e^{\frac{\pi D}{4\delta}}}{\pi D} \quad (3A)$$

This simple exponential expression, which is identical to Equation 2A in the upper and lower limits, is a good approximation to Equation 2A and can be considered to be an extension of the approximation formula presented for the isotropic case [3] to the collimated case.

REFERENCES

1. Geronemus RG, Quintana AT, Lou WW, Kauvar AN. High-fluence modified pulsed dye laser photocoagulation with dynamic cooling of port-wine stains in infancy. Arch Dermatol 2000;136:942–943.
2. Lanigan SW. Port-wine stains unresponsive to pulsed dye laser: Explanations and solutions. Br J Dermatol 1998;139: 173–177.
3. Svaasand LO, Fiskerstrand EJ, Kopstad G, Norvang LT, Svaasand EK, Nelson JS, Berns MW. Therapeutic response during pulsed laser treatment of port-wine stains; dependence on vessel diameter and depth in dermis. Lasers Med Sci 1995;10:235–243.
4. Alam M, Dover JS, Arndt KA. Treatment of facial telangiectasia with variable-pulse high-fluence pulsed-dye laser: Comparison of efficacy with fluences immediately above and below the purpura threshold. Dermatol Surg 2003;29:681–684.
5. Chang CJ, Kelly KM, Nelson JS. Cryogen spray cooling and pulsed dye laser treatment of cutaneous hemangiomas. Ann Plast Surg 2001;46:577–583.
6. Anderson RR, Parrish JA. Selective photothermolysis: Precise microsurgery by selective absorption of pulsed radiation. Science 1983;220(4596):524–527.
7. van Gemert MJC, Welch AJ, Pickering JW, Tan OT, Gijsbers GH. Wavelengths for laser treatment of port wine stains and telangiectasia. Lasers Surg Med 1995;16:147–155.
8. Kimel S, Svaasand LO, Hammer-Wilson MJ, Nelson JS. Influence of wavelength on response to laser photothermolysis of blood vessels: Implications for port wine stain laser therapy. Lasers Surg Med 2003;33:288–295.
9. Kimel S, Svaasand LO, Hammer-Wilson M, Schell MJ, Milner TE, Nelson JS, Berns MW. Differential vascular response to laser photothermolysis. J Invest Dermatol 1994; 103:693–700.
10. Nelson JS, Milner TE, Svaasand LO, Kimel S. Laser pulse duration must match the estimated thermal relaxation time for successful photothermolysis of blood vessels. Lasers Med Sci 1995;10:9–12.
11. Kimel S, Svaasand LO, Cao D, Hammer-Wilson MJ, Nelson JS. Vascular response to laser photothermolysis as a function of pulse duration, vessel type, and diameter: Implications for port wine stain laser therapy. Lasers Surg Med 2002;30:160–169.
12. Dierickx CC, Casparian JM, Venugopalan V, Farinelli WA, Anderson RR. Thermal relaxation of port-wine stain vessels probed in vivo: The need for 1–10 millisecond laser pulse treatment. J Invest Dermatol 1995;105:709–714.
13. de Boer JF, Lucassen GW, Verkruysse W, van Gemert MJC. Thermolysis of port-wine-stain blood vessels: Diameter of a damaged blood vessel depends on the laser pulse length. Lasers Med Sci 1996;11:177–180.
14. Altshuler GB, Anderson RR, Manstein D, Zenzie HH, Smirnov MZ. Extended theory of selective photothermolysis. Lasers Surg Med 2001;29:416–432.
15. Lucassen GW, Svaasand LO, Verkruysse W, van Gemert MJC. Laser energy threshold for thermal vascular injury in a port-wine stain skin model. Lasers Med Sci 1995;10: 231–234.
16. Pfefer TJ, Choi B, Vargas G, McNally KM, Welch AJ. Pulsed laser-induced thermal damage in whole blood. J Biomech Eng 2000;122:196–202.
17. Tan OT, Morelli JG, Whitaker D, Boll J, Murphy G. Ultrastructural changes in red blood cells following pulsed irradiation in vitro. J Invest Dermatol 1989;92:100–104.
18. Verkruysse W, Nilsson AMK, Milner TE, Beek JF, Lucassen GW, van Gemert MJC. Optical absorption of blood depends on temperature during a 0.5 ms laser pulse at 586 nm. Photochem Photobiol 1998;67:276–281.
19. Black JF, Barton JK. Chemical and structural changes in blood undergoing laser photocoagulation. Photochem Photobiol 2004;80:89–97.
20. Verkruysse W, Beek JF, VanBavel E, van Gemert MJC, Spaan JA. Laser pulse impact on rat mesenteric blood vessels in relation to laser treatment of port wine stain. Lasers Surg Med 2001;28:461–468.
21. Barton JK, Vargas G, Pfefer TJ, Welch AJ. Laser fluence for permanent damage of cutaneous blood vessels. Photochem Photobiol 1999;70:916–920.
22. Barton JK, Hammer DX, Pfefer TJ, Lund DJ, Stuck BE, Welch AJ. Simultaneous irradiation and imaging of blood vessels during pulsed laser delivery. Lasers Surg Med 1999; 24:236–243.
23. Barton JK, Frangineas G, Pummer H, Black JF. Cooperative phenomena in two-pulse, two-color laser photocoagulation of cutaneous blood vessels. Photochem Photobiol 2001;73:642–650.
24. Barton JK, Rollins A, Yazdanfar S, Pfefer TJ, Westphal V, Izatt JA. Photothermal coagulation of blood vessels: A comparison of high-speed optical coherence tomography and numerical modelling. Phys Med Biol 2001;46:1665–1678.
25. Suthamjariya K, Farinelli WA, Koh W, Anderson RR. Mechanisms of microvascular response to laser pulses. J Invest Dermatol 2004;122:518–525.
26. Randeberg LL, Bonesronning JH, Dalaker M, Nelson JS, Svaasand LO. Methemoglobin formation during laser induced photothermolysis of vascular skin lesions. Lasers Surg Med 2004;34:414–419.
27. Nilsson AMK, Lucassen GW, Verkruysse W, Andersson-Engels S, van Gemert MJC. Changes in optical properties of human whole blood in vitro due to slow heating. Photochem Photobiol 1997;65:366–373.
28. Jansen ED, Asshauer T, Frenz M, Motamedi M, Delacretaz G, Welch AJ. Effect of pulse duration on bubble formation and laser-induced pressure waves during holmium laser ablation. Lasers Surg Med 1996;18:278–293.
29. van Leeuwen TG, Jansen ED, Welch AJ, Borst C. Excimer laser induced bubble: Dimensions, theory, and implications for laser angioplasty. Lasers Surg Med 1996;18:381–390.
30. Cain CP, Noojin GD, Manning LW. A comparison of various probit methods for analyzing yes/no data on a log scale. Technical Report USAF AL/OE-TR-1996-0102 (1996).
31. Zijlstra WG, Buursma A, van Assendelft OW. Visible and near infrared absorption spectra of human and animal haemoglobin determination and application. The Netherlands: VSP, Zeist, 2000.
32. Carslaw HS, Jaeger JC. Conduction of heat in solids, 2nd edn. Oxford: Clarendon Press, 1959.
33. Incropera FP, DeWitt DP. Fundamentals of heat and mass transfer. New York: John Wiley & Sons, 1996.